

УДК 621:664: 669.01(075)

THICKNESS INFLUENCE ON ELEMENT SEGREGATION IN CONTINUOUSLY CAST STEEL SLABS

Y. G. Aftandilians

National University of Life and Environmental Sciences of Ukraine, Ukraine.

Speciality of article: 131 – applied mechanics.

Corresponding author: aftyev@yahoo.com.

Article history: Received – January 2021, Accepted – June 2021, Published – 30 July 2021.

Bibl. 9, fig. 4, tabl. 8.

Abstract. The article presents the results of a study of the effect of slab thickness on the element segregation of during continuous casting of billets. The process of accumulation of elements on the surface of dendrites during crystallization of steel slabs for various thicknesses is considered. The theoretical dependence of the process of accumulation of elements on the dendrite surface during the crystallization of steel slabs for various thicknesses has been established. It is shown that the efficiency of accumulation of elements on the dendrite surface depends significantly from the crystallization and cooling rate of the slab.

The established dependence makes it possible to determine the permissible increased element content in strips, which is equivalent to their content in thick slabs during continuous casting of billets. The element segregation searching shows that at pouring of thin steel strips, an increasing of the element content is possible compared to continuous casting of thick slabs with an identical level of segregation.

The elements are arranged as possible to maximize the impurities content in AISI 1006 carbon steel in the following decreasing sequence: S, O, N, P, H. Another sequence is observed for stainless steel AISI 304: O, S, P, H, N.

The following sequences are observed in the case of residual elements: for steel AISI 1006 - Pb, Bi, Sn, As, Zn, Sb, Cu; for steel AISI 304 - Cu, Sb, Sn, Bi, Pb, As, Zn.

The sequences are as follows for the alloying elements: for steel AISI 1006 - B, Se, Al, Te, Ca, Mg, Ce, C, La, Nb, Ti, Mn, Ni, Si, Cr; for steel AISI 304 - Ca, Te, Al, Ti, Mg, C, La, Ce, Nb, Se, V, B, Si, Cr, Mn.

Key words: segregation, steel, chemical composition, austenite, δ-ferrite, element distribution, dendrite, liquid, solid, phase.

Introduction

Continuous casting technology is one of the economical ways to produce high quality billets. The world's leading manufacturers produce by continuous casting from 81 to 97% of the total steel production [1].

Approximately 2/3 of the total steel volume is produced on slab continuous casting machines for sheet production.

Currently, there is a tendency in the world to transition from the manufacture of thick-sheet (150-300 mm) [1] to thin-sheet (1-5 mm) [2] continuously cast blanks.

This is due to the fact that when pouring of billets with dimensions close to the final, the number of technological operations decreases, capital and energy costs are reduced, and the working cycle is reduced.

Formulation of problem

A thickness decreasing accompanies by a change of the conditions of the structure formation and the development of chemical and structural heterogeneity in the sheet during continuously casting of steel slabs. However, systemic studies of the peculiarities of the structure formation and the development of chemical and structural heterogeneity of thin strip have been insufficiently performed.

Therefore, the problem of studying the features of the segregation process of elements during the formation of thin strip at continuously casting is current importance.

Analysis of recent research results

The segregation of elements in metal, generally for the equilibrium conditions, depend on the temperature and the elements solubility in solid and liquid. It is characterized by the equilibrium coefficient of elements distribution (k_{oi}). In non-equilibrium conditions a very strong influence exert on these phenomena the forming condition of dendrite structure and the secondary structure.

The element segregation during the dendrite structure forming depend mainly on:

- element solubility in solid and liquid phases;
- crystallization rate (v_{cr});
- mobility diffusion time of elements (D);
- dendrite size (x^p);

- kinematic viscosity of liquid phase (ν);
- velocity of liquid metal around the dendrites (u_∞).

Table 1. Distribution of elements between liquid and solid phases for equilibrium conditions.

Element	Atomic mass, M	Iron type	Transformation t, °C	Solubility, % wt.		k _{oi}
				in solid	in liquid	
Impurities						
H	1.0079	δ	1535	0.00108	0.00253	0.43
		γ	1401	0.00045	0.0009	0.50
N	14.007	δ	1536	0.01	0.0451	0.22
		γ	650	0.702	1.141	0.62
O	15.999	δ	1536	0.00344	0.0458	0.08
		γ	1528	0.000869	0.00344	0.25
P	30.974	δ	1048	2.384	9.425	0.25
		γ	1150	0.249	0.499	0.50
S	32.060	δ	1365	0.175	11.285	0.02
		γ	1365	0.051	0.175	0.29
Alloying elements						
C	12.011	δ	1498	0.101	0.497	0.20
		γ	1153	1.978	3.719	0.53
Si	28.086	δ	1250	10.05	12.57	0.8
		γ	1150	1.96	1.96	1.0
Mn	54.938	δ	1473	9.44	12.78	0.74
		γ	1244	100	100	1.00
Cr	51.996	δ	1507	21.41	21.41	1
		γ	830	6.98	6.98	1
V	50.9414	δ	1468	30.09	30.09	1
		γ	1150	1.28	1.82	0.70
Ni	58.71	δ	1512	3.993	5.465	0.73
		γ	1450	100	100	1
Nb	92.906	δ	1372	4.656	17.628	0.26
		γ	1150	1.663	2.66	0.62
B	10.81	δ	1381	0.00135	1.393	0.00097
		γ	1381	0.00116	0.00135	0.86
Mg	24.305	δ	1515	0.087	0.753	0.125
		γ	1388	0.0435	0.087	0.500
Al	25.9815	δ	1232	24.65	0.0744	0.075
		γ	1160	0.721	0.00558	0.250
Ca	40.08	δ	1538	0.00395	0.0323	0.12
		γ	1392	0.0179	0.0358	0.05
Ti	47.9	δ	1289	8.4	13.72	0.61
		γ	1100	0.171	0.514	0.33
La	138.906	δ	1400	4.973	24.864	0.20
		γ	1382	0.137	0.249	0.55
Ce	140.12	δ	1390	3.511	27.59	0.127
		γ	1390	0.0376	0.0627	0.600
Residual elements						
Cu	63.546	δ	1478	7.62	11.716	0.650
		γ	1094	8.53	99	0.078
Zn	65.38	δ	780	50.32	99	0.48
		γ	1150	0.0655	0.076	0.85
Sn	118.69	δ	1128	17.63	64.37	0.27
		γ	1150	1.7	3.19	0.53
Pb	207.19	δ	1535	0.001	0.0482	0.021
		γ	1391	0.167	0.260	0.650
Bi	208.98	δ	1538	0.0112	0.0935	0.12
		γ	1391	0.206	0.374	0.55

The element accumulation on boundary surface between the solid and liquid phases, for equilibrium conditions, depend on the state diagrams Fe-I (element) and the value of the equilibrium distribution coefficient (k_{oi} = percentage ration of element I in solid iron and liquid iron) in iron.

This coefficient for equilibrium conditions has the following values as presented in table 1 [3-5].

The data of table 1 are the basis for calculating and predicting of the thickness influence on the element segregation in continuously cast steel slabs.

Purpose of research

The purpose of the work is the theoretical and methodological substantiation to investigate the influence of slabic thickness on the segregation of elements during continuous casting of preparations.

Research results

The element heterogeneity during the first time of equilibrium crystallization (without diffusion) in δ and γ fields is shown in table 2.

Table 2. Solubility ratio of elements in liquid and solid iron (C_{liq}/C_{isol}) in the first time of equilibrium crystallization of iron in δ and γ fields.

Element	C_{liq}/C_{isol}		Element t	C_{liq}/C_{isol}	
	δ - iron	γ - iron		δ - iron	γ - iron
Residual elements					
Pb	47.62	1.54	S	62.50	3.45
Bi	8.33	1.82	O	13.33	4.00
Sn	3.70	1.89	N	4.55	1.61
As	2.56	1.35	P	4.00	2.00
Zn	2.08	1.18	H	2.33	2.00
Sb	2.00	2.33			
Cu	1.54	12.82			
Alloying elements					
B	1030.9	1.16	Ti	1.64	3.03
C	5.00	1.89	Cr	1.00	1.00
Mg	8.00	2.00	V	1.00	1.43
Al	13.33	4.00	Mn	1.35	1.00
Si	1.25	1.00	Ni	1.37	1.00
Ca	8.33	20.00	Nb	3.85	1.61
La	5.00	1.82	Se	50.00	1.49
Ce	7.87	1.67	Te	10.00	16.13

Data of table 2 show that the crystallization of iron in δ -phase present more heterogeneity during first time of crystallization:

- for residual elements – Pb is first (Pb will be 47.62 times more on boundary surface between the solid and liquid phase than in liquid metal) and less for other residual elements Bi, Sn, As, Zn, Sb, Cu;

- for impurities – S is first (S will be 62.5 times more on boundary surface between the solid and liquid

phase than in liquid metal)) and less for other impurities O, N, P, H;

- for alloying elements – B is first (B will be 1031 times more on boundary surface between the solid and liquid phase than in liquid metal)) and less for other alloying elements Se, Al, Te, Ca, Mg, Ce, La, C, Nb, Ti, Ni, Mn, Si, Cr, V.

Instead, for crystallization in γ -phase it is:

- for residual elements – Cu is first (Cu will be 12.82 times more on boundary surface between the solid and liquid phase than in liquid metal)) and less for other residual elements Sb, Sn, Bi, Pb, As, Zn;

- for impurities – O is first (O will be 4 times more on boundary surface between the solid and liquid phase than in liquid metal)) and less for other impurities S, P, H, N;

- for alloying elements – Ca is first (Ca will be 20 times more on boundary surface between the solid and liquid phase than in liquid metal)) and less for other alloying elements Te, Al, Ti, Mg, C, La, Ce, Nb, Se, V, B, Ni, Mn, Si, Cr.

The effective coefficient of element distribution (k_{eff}), in non-equilibrium conditions, has the next dependence [3]:

$k_{eff} = k_{oi}/(k_{oi} + (1 - k_{oi})\exp(-v_{cr} \cdot \delta_c/D))_{fp}$, (1)

where k_{oi} – the equilibrium coefficient of elements distribution, v_{cr} – crystallization rate, δ_c – diffusion boundary layer, D – coefficient of element diffusion (usually in melt iron is $D = 5 \cdot 10^{-9} \div 1 \cdot 10^{-8} \text{ m}^2/\text{s}$ [3])

The thickness of the diffusion layer (δ_c) around dendrites is found according to next formula:

$$\delta_c = \delta/1.026 \cdot (v/D)^{1/3}, \quad (2)$$

the thickness of boundary layer (δ) in the above formula is expresed as follow:

$$\delta = 4.64 \cdot (x^p \cdot v/u_\infty)^{1/2}, \quad (3)$$

where x^p – distance between the dendrite peak, v – kinematic viscosity of melt, u_∞ – laminar movement speed of melt flow.

In fig. 1 is shown the velocity distribution of the melt flow around the dendrite.

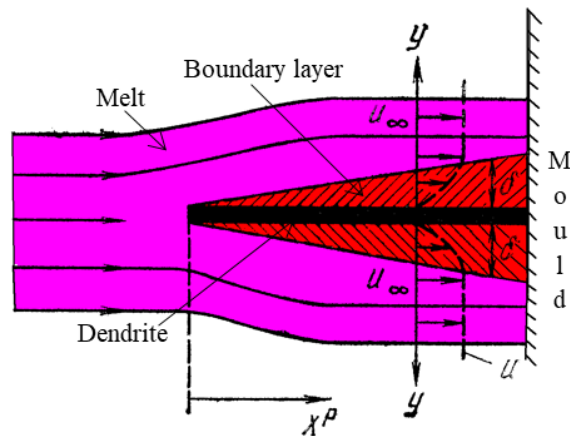


Fig. 1. Velocity distribution of melt flow nearest to the dendrite [6].

Strip and thick slab parameters are shown in table 3. The boundary and diffusion layers are calculated, for

the processes of strip and thick slab casting in the table 4, according to the data presented in table 3.

Table 3. Strip and thick slab parameters.

Parameter	Strip	Thick slab
Thickness, mm	1.2	1.8
Casting speed, m/min	131	59
Total solidification time, s	0.116	0.258
Average speed of crystallization, mm/s	5.172	3.488
Average shell cooling rate in mould, °C/s	1853	826
Average size of dendrites (x_p), mm	0.6 - 0.7	1.0 - 1.2
Speed of melt flow (u_∞), m/s	0.2 - 0.50	0.2 - 0.6
Coefficient of diffusion of elements (D), m ² /s	$5 \cdot 10^{-9} \div 1 \cdot 10^{-8}$	
Kinematic viscosity of melt, with C = 0.054 % wt., at 1550 °C (v), m ² /s	$10.8 \cdot 10^{-7}$	

Table 4. Values of the boundary (δ) and diffusion layers (δ_c) and the parameter $v_{cr} \cdot \delta_c / D$ for the processes of strip and thick slab casting.

Parameter	Type of slab		
	Thick	Strip	
	Thickness, mm	220	1.8
δ , mm	min	0.68	0.22
	max	1.53	0.37
δ_c , mm	min	0.110	0.035
	max	0.312	0.077
	average	0.211	0.056
$v_{cr} \cdot \delta_c / D$	min	2.27	24.4
	max	3.21	26.68
	average	2.74	25.55

It is observed that from the table 4 the thickness of the diffusion layer (δ_c) for strip casting is 3.78 to 4.94 times less than for the conventional continuous casting and the integral parameter ($v_{cr} \cdot \delta_c / D$) increases from 9.32 to 10.59 times. This means that for the strip casting the value of the distribution coefficients increases as shown in figure 2.

Increasing of the value of the effective coefficient of element distribution (k_{eff}) must increase the steel homogeneity in diffusion layer (C_{δ_c}), due to the accumulation of elements on interface dendrites/liquid steel, that could be calculated by the following formula.

$$C_{\delta_c} = C_{liq} \left(1 + \frac{1 - k_{eff}}{k_{eff} \cdot \exp \left(\frac{v_{cr} \cdot \delta_c}{D} \right)} \right), \quad (4)$$

The maximum accumulation of elements is for the conditions: $\delta_c = 0$ and $C_{\max} = C_{liq}/k_{eff}$ (fig. 3).

Calculations of the effective coefficient of element distribution (k_{eff}) and maximum segregation of elements (C_{liq}/k_{eff}) are shown in table 5.

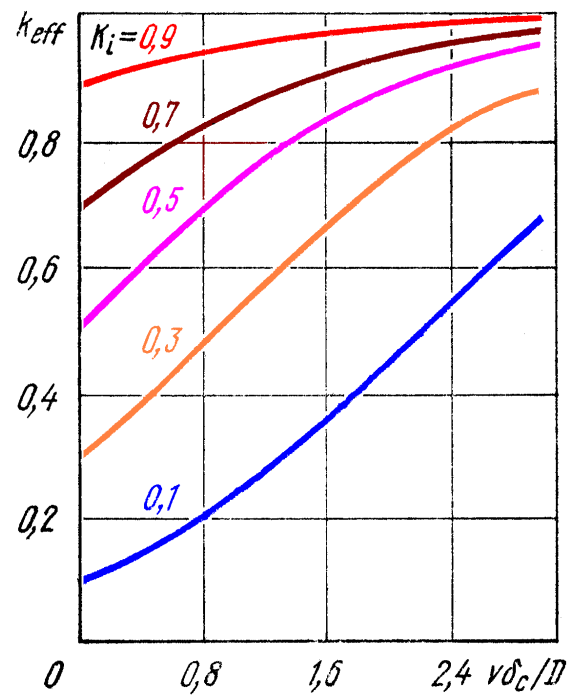


Fig. 2. Dependence of k_{eff} from of the parameter $(v_{cr} \cdot \delta_c / D)$.

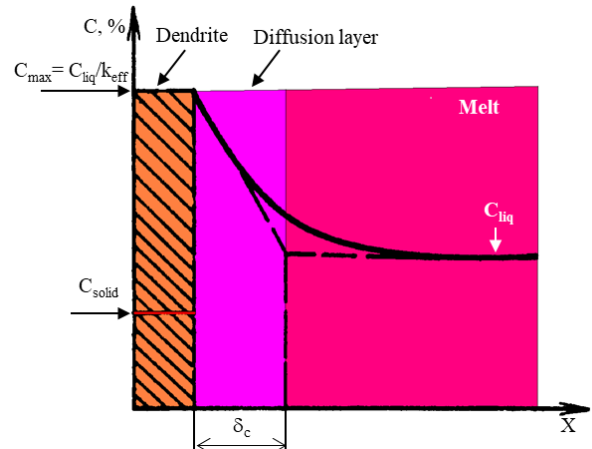


Fig. 3. Distribution of elements on interface dendrite/liquid steel.

The data of the table 5 show that the increasing of the cooling and crystallization rate decreases the micro segregation of steels, and for the strip casting the transformation of liquid to solid takes place practically without diffusion, keeping the liquid state.

Experimental data presented in [7-9] table 6, 7 confirm the above calculations (fig. 4).

The dendrite segregation in conventional continuous casting is next: S = 1.8 - 2.4, C = 1.45 - 1.7, Cr = 1.25 - 1.75, Mn = 1.2 - 1.45, Ni = 1.2 - 1.35 [9].

Instead, for the strip casting the segregation index aspires to 1. For example, the segregation index for as-cast strip (AISI 304 stainless steel) is next [10]: Cr = 1, Ni = 0.99, Mn = 0.98, Si = 1.

$$C_{\max(i)} = C_{liq(i)} \cdot \left(1 + \frac{1 - k_{eff}}{k_{eff(i)}} \right) = C_{liq(i)}/k_{eff(i)}, \quad (5)$$

For conventional casting

$$C_{\max(conv)(i)} = C_{liq(conv)(i)}/k_{eff(conv)(i)}, \quad (6)$$

and strip casting

$C_{\max(\text{strip})(i)} = C_{\text{liq}(\text{strip})(i)}/k_{\text{eff}(\text{strip})(i)}$, (7)
 where $C_{\text{liq}(\text{conv})(i)}$ is the content of element I in liquid steel for the conventional continuous casting, $C_{\text{liq}(\text{strip})(i)}$ is the content of element I in liquid steel for the strip casting, $k_{\text{eff}(\text{conv})(i)}$ is the effective coefficient of distribution of element I for the conventional continuous casting, $k_{\text{eff}(\text{strip})(i)}$ is the effective coefficient of distribution of element I for strip casting.

Table 5. Effective coefficient of element distribution (k_{eff}) and maximum segregation of elements ($C_{\text{liq}}/k_{\text{eff}}$) respectively for thick slab and strip casting.

C i	Strip casting (thickness - 1.8 mm)				Thick slab (thickness - 220 mm)			
	δ - iron		γ - iron		δ - iron		γ - iron	
	k_e ff	$C_{\text{liq}}/k_{\text{eff}}$	k_e ff	$C_{\text{liq}}/k_{\text{eff}}$	k_e ff	$C_{\text{liq}}/k_{\text{eff}}$	k_e ff	$C_{\text{liq}}/k_{\text{eff}}$
Impurities								
H	1	0.003	1	0.001	0.92	0.003	0.94	0.001
N	1	0.045	1	1.141	0.81	0.055	0.96	1.186
O	1	0.046	1	0.003	0.56	0.082	0.84	0.004
P	1	9.425	1	0.499	0.84	11.25	0.94	0.531
S	1	11.29	1	0.175	0.20	56.10	0.86	0.203
Residual elements								
Zn	1	99	1	0.076	0.94	100.0	0.99	0.077
Sn	1	64.37	1	3.19	0.85	75.63	0.95	3.372
Pb	1	0.048	1	0.260	0.25	0.193	0.97	0.269
Alloying elements								
B	1	1.39	1	0.001	0.02	94.03	0.99	0.001
C	1	0.50	1	3.72	0.8	0.62	0.9	3.93
Mg	1	0.75	1	0.09	0.7	1.09	0.9	0.09
Al	1	0.07	1	0.01	0.6	0.13	0.8	0.01
Si	1	12.6	1	1.96	0.98	12.8	1.0	1.96
Ca	1	0.03	1	0.04	0.77	0.05	0.44	0.08
Ti	1	13.7	1	0.51	0.96	14.28	0.88	0.58
Cr	1	21.4	1	6.98	1.0	21.4	1.0	6.98
V	1	30.1	1	1.82	1.0	30.09	0.97	1.870
Mn	1	12.8	1	100	0.98	13.0	1.0	100
Ni	1	5.47	1	100	0.98	5.59	1.0	100
Nb	1	17.6	1	2.66	0.8	20.9	0.96	2.77
La	1	24.9	1	0.25	0.80	31.3	0.95	0.26
Ce	1	27.6	1	0.06	0.7	39.8	0.96	0.07
Se	1	7.07	1	0.21	0.2	29.4	0.97	0.22
Te	1	2.28	1	0.38	0.6	3.60	0.5	0.72

Table 6. Dendrites elements segregation in ingots [7].

Element	Ratio of content element I in between arm spacing of dendrites to content element I in arm dendrites, $C_{\Delta 2}/C_d$
S	1.50 – 2.00
P	1.47 – 1.65
C	1.45 – 1.60
W	1.60 – 1.70
As	1.40 – 1.60
V	1.30 – 1.50
Mo	1.25 – 1.45
Si	1.17 – 1.23
Cr	1.17 – 1.23
Mn	1.12 – 1.18
Ni	1.00 – 1.10

In case of considering equal segregation for both processes of conventional continuous casting and of strip casting the following conditions will be verified:

$$C_{\max(\text{conv})(i)} = C_{\max(\text{strip})(i)}, \quad (8)$$

$$\frac{C_{\text{liq}(\text{conv})(i)}}{k_{\text{eff}(\text{conv})(i)}} = \frac{C_{\text{liq}(\text{strip})(i)}}{k_{\text{eff}(\text{strip})(i)}}, \quad (9)$$

$$C_{\text{liq}(\text{strip})(i)} = C_{\text{liq}(\text{conv})(i)} \cdot \frac{k_{\text{eff}(\text{strip})(i)}}{k_{\text{eff}(\text{conv})(i)}}, \quad (10)$$

Table 7. Segregation ratio of as-cast strip [8].

Elements	After mould roll pressing force, ton			
	0	2.3	20.5	38.8
Cr	0.99	0.99	1.0	1.0
Ni	0.98	0.95	0.89	0.88
Mn	0.97	0.94	0.90	0.80

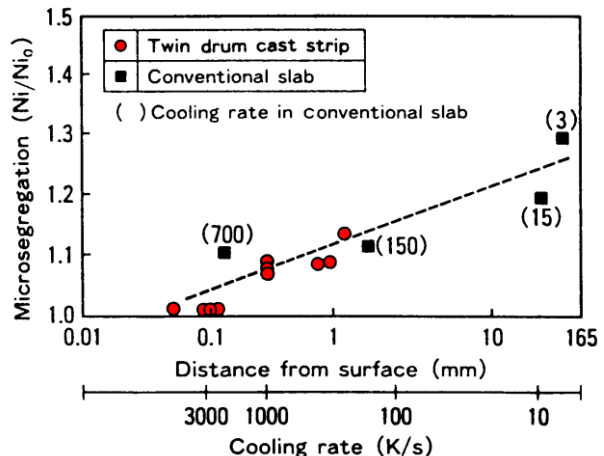


Fig. 4. Influence of cooling rate on micro segregation of Ni for AISI 304 stainless steel.

In according with formula 4 the maximum elements segregation of element I ($C_{\max(i)}$) will be at $\delta_c = 0$ (see fig. 3).

The ratio $k_{\text{eff}(\text{strip})(i)}/k_{\text{eff}(\text{conv})(i)}$ shows how many times is possibility to increase the element content in liquid steel, for the strip casting process, maintaining the same segregation index as for the conventional continuous casting. Results of calculation are presented in table 8.

The data presented in table 8 shown that maximum possible increase of elements in carbon (AISI 1006) and stainless (AISI 304) steels for the strip casting process (considering a thickness of 1.8 mm) in comparison with the continuous casting process (considering a thickness of 220 mm) for the conditions of having equal dendrite segregation for the both processes are different.

The elements are arranged as possible to maximize the impurities content in AISI 1006 carbon steel in the following decreasing sequence: S, O, N, P, H. Another sequence is observed for stainless steel AISI 304: O, S, P, H, N.

The following sequences are observed in the case of residual elements:

- for steel AISI 1006 - Pb, Bi, Sn, As, Zn, Sb, Cu;
- for steel AISI 304 - Cu, Sb, Sn, Bi, Pb, As, Zn.

Table 8. Theoretical possibility of increasing the element percentage in liquid steel for the strip casting process (considering a thickness of 1.8 mm) in comparison with the continuous casting process (considering a thickness of 220 mm) for the conditions of having equal dendrite segregation for the both processes.

Percentage increase of elements, % (This percentage is compared to the element level for the conventional continuous casting)			
Crystallization in δ phase (For example steel AISI 1006)		Crystallization in γ phase (For example steel AISI 304)	
Impurities			
S	497.1	O	19.4
O	79.6	S	15.8
N	22.9	P	6.5
P	19.4	H	6.5
H	8.6	N	4.0
Residual elements			
Pb	401.0	Cu	76.3
Bi	47.4	Sb	8.6
Sn	17.5	Sn	5.7
As	10.1	Bi	5.3
Zn	7.0	Pb	3.5
Sb	6.5	As	2.3
Cu	3.5	Zn	1.1
Alloying elements			
B	6750.3	Ca	222.7
Se	416.4	Te	97.7
Al	79.6	Al	19.4
Te	58.1	Ti	13.1
Ca	47.4	Mg	6.5
Mg	45.2	C	5.7
Ce	44.4	La	5.3
C	25.8	Ce	4.3
La	25.8	Nb	4.0
Nb	18.4	Se	3.2
Ti	4.1	V	2.8
Mn	2.3	B	1.1
Ni	2.3	Si	0
Si	1.6	Cr	0
Cr	0	Mn	0

The sequences are as follows for the alloying elements:

- for steel AISI 1006 - B, Se, Al, Te, Ca, Mg, Ce, C, La, Nb, Ti, Mn, Ni, Si, Cr;
- for steel AISI 304 - Ca, Te, Al, Ti, Mg, C, La, Ce, Nb, Se, V, B, Si, Cr, Mn.

Conclusions

1. The established dependence makes it possible to determine the permissible increased content of elements in steel strips, in comparison with thick slabs, at which their level of segregation is equivalent to the level of their segregation in thick slabs during continuous casting of billets.

2. Research on the micro segregation of elements has shown that for the strip casting process the element content could be increased too much in steel compared to the conventional slab casting having the same level of the micro segregation.

3. The elements are arranged as possible to maximize the impurities content in AISI 1006 carbon steel in the following decreasing sequence: S, O, N, P, H. Another sequence is observed for stainless steel AISI 304: O, S, P, H, N.

4. The following sequences are observed in the case of residual elements:

- for steel AISI 1006 - Pb, Bi, Sn, As, Zn, Sb, Cu;
- for steel AISI 304 - Cu, Sb, Sn, Bi, Pb, As, Zn.

5. The sequences are as follows for the alloying elements:

- for steel AISI 1006 - B, Se, Al, Te, Ca, Mg, Ce, C, La, Nb, Ti, Mn, Ni, Si, Cr;
- for steel AISI 304 - Ca, Te, Al, Ti, Mg, C, La, Ce, Nb, Se, V, B, Si, Cr, Mn.

Список літератури

1. *Zhi-ling Peng, Chun-gui Zhou.* Research on modeling of nonlinear vibration isolation system based on Bouc-Wen model. Defence Technology. 2014. Vol. 10. P. 371-374.
2. *Semenov M. E., Meleshenko P. A., Solovyov A. M., Semenov A. M.* Hysteretic nonlinearity in inverted pendulum problem. Springer Proceedings in Physics. 2015. Vol. 168. P. 463-507.
3. *Bernyk I., Nazarenko I., Luhovskyi O.* Effect of rheological properties of materials on their treatment with ultrasonic cavitation. Materials and technology. 2018. Vol. 4 (52). P. 465-468.
4. *Veklich A., Tmenova T., Zazimko O., Trach V., Lopatko K., Titova L., Boretskij V., Aftandiliants Y., Lopatko S., Rogovskiy I.* Regulation of biological processes with complexions of metals produced by underwater spark discharge. 2020. Springer Proceedings in Physics. Book series Nanomaterials and Nanocomposites, Nanostructure Surfaces and Their Applications. Vol. 247. P. 283-306.
5. *Nazarenko I., Dedov O., Bernyk I., Rogovskii I., Bondarenko A., Zapryvoda A., Titova L.* Study of stability of modes and parameters of motion of vibrating machines for technological purpose. Eastern-European Journal of Enterprise Technologies. 2020. Vol. 6 (7-108). P. 71-79. doi: 10.15587/1729-4061.2020.217747.
6. *Hrynkiv A., Rogovskii I., Aulin V., Lysenko S., Titova L., Zagurskiy O., Kolosok I.* Development of a system for determining the informativeness of the diagnosing parameters of the cylinder-piston group of the diesel engines in operation. Eastern-European Journal of Enterprise Technologies. 2020. Vol. 3(105). P. 19-29.
7. *Tmenova T., Valensi F., Veklich A., Cressault Y., Boretskij V., Lopatko K., Aftandilyant Y.* Etude d'un arc impulsif immergé à l'aide de deux dispositifs expérimentaux. Journal International de Technologie, de l'Innovation, de la Physique, de l'Energie et de

l'Environnement. 2017. Vol. 3. No 1. P. 2428-8500. doi: 10.18145/jitipee.v3i1.159.

8. Loveikin V., Romasevych Y., Shymko L., Ohiienko M., Duczmal W., Potwora W., Titova L., Rogovskii I. Agrotronics and optimal control of cranes and hoisting machines: monograph. Opole: The Academy of Management and Administration in Opole. 2020. 164 p.

9. Boretskij V. F., Veklich A. N., Tmenova T. A., Cressault Y., Valensi F., Lopatko K. G., Aftandilyants Y. G. Plasma of underwater electric discharges with metal vapors. Problems of atomic science and technology. 2019. № 1. Series: Plasma Physics (25). P. 127-130.

References

1. Zhi-ling Peng, Chun-gui Zhou. (2014). Research on modeling of nonlinear vibration isolation system based on Bouc-Wen model. Defence Technology. 10. 371-374.

2. Semenov M. E., Meleshenko P. A., Solovyov A. M., Semenov A. M. (2015). Hysteretic nonlinearity in inverted pendulum problem. Springer Proceedings in Physics. 168. 463-507.

3. Bernyk I., Nazarenko I., Luhovskyi O. (2018). Effect of rheological properties of materials on their treatment with ultrasonic cavitation. Materials and technology. 4 (52). 465-468.

4. Veklich A., Tmenova T., Zazimko O., Trach V., Lopatko K., Titova L., Boretskij V., Aftandiliants Y., Lopatko S., Rogovskiy I. (2020). Regulation of biological processes with complexions of metals produced by underwater spark discharge. Springer Proceedings in Physics. Book series Nanomaterials and Nanocomposites, Nanostructure Surfaces and Their Applications. 247. 283-306.

5. Nazarenko I., Dedov O., Bernyk I., Rogovskii I., Bondarenko A., Zapryvoda A., Titova L. (2020). Study of stability of modes and parameters of motion of vibrating machines for technological purpose. Eastern-European Journal of Enterprise Technologies. 6 (7-108). 71-79. doi: 10.15587/1729-4061.2020.217747.

6. Hrynkiv A., Rogovskii I., Aulin V., Lysenko S., Titova L., Zagurskiy O., Kolosok I. (2020). Development of a system for determining the informativeness of the diagnosing parameters of the cylinder-piston group of the diesel engines in operation. Eastern-European Journal of Enterprise Technologies. 3(105). 19-29.

7. Tmenova T., Valensi F., Veklich A., Cressault Y., Boretskij V., Lopatko K., Aftandilyant Y. (2017). Etude d'un arc impulsif immergé à l'aide de deux dispositifs expérimentaux. Journal International de Technologie, de l'Innovation, de la Physique, de l'Energie et de l'Environnement. 3(1). 2428-8500. doi: 10.18145/jitipee. v3i1.159.

8. Loveikin V., Romasevych Y., Shymko L., Ohiienko M., Duczmal W., Potwora W., Titova L., Rogovskii I. (2020). Agrotronics and optimal control of cranes and hoisting machines: monograph. Opole: The Academy of Management and Administration in Opole. 164.

9. Boretskij V. F., Veklich A. N., Tmenova T. A., Cressault Y., Valensi F., Lopatko K. G., Aftandilyants Y. G. (2019). Plasma of underwater electric discharges with metal vapors. Problems of atomic science and technology. 1. Series: Plasma Physics (25). 127-130.

ВЛИЯНИЕ ТОЛЩИНЫ СЛЯБОВ НА СЕГРЕГАЦИЮ ЭЛЕМЕНТОВ ПРИ НЕПРЕРЫВНОМ ЛИТЬЕ ЗАГОТОВОК Е. Г. Афтандилянц

Аннотация. В статье приводятся результаты исследования влияния толщины слябов на сегрегацию элементов при непрерывном литье заготовок. Рассмотрен процесс накопления элементов на поверхности дендритов при кристаллизации стальных слябов различной толщины. Установлена теоретическая зависимость процесса накопления элементов на поверхности дендритов существенно зависит от скорости кристаллизации и охлаждения сляба. Установленная зависимость позволяет определить допустимое повышенное содержание элементов в лентах, эквивалентное их содержанию в толстых слябах при непрерывном литье заготовок. Исследование сегрегации элементов показало, что при разливки тонких стальных лент возможно увеличение содержания элементов по сравнению с непрерывной разливкой толстых слябов при идентичном уровне сегрегации.

По уровню максимального увеличения содержания примесей в тонких лентах из углеродистой стали AISI 1006 элементы располагаются в следующей убывающей последовательности: S, O, N, P, H. Для тонких лент из нержавеющей стали AISI 304 наблюдается другая последовательность: O, S, P, H, N.

В случае остаточных элементов наблюдаются следующие закономерности:

- для ленты из стали AISI 1006 - Pb, Bi, Sn, As, Zn, Sb, Cu;

- ленты из стали AISI 304 - Cu, Sb, Sn, Bi, Pb, As, Zn.

Для легирующих элементов установленные последовательности имеют следующий вид:

- ленты из стали AISI 1006 - B, Se, Al, Te, Ca, Mg, Ce, C, La, Nb, Ti, Mn, Ni, Si, Cr;

- ленты из стали AISI 304 - Ca, Te, Al, Ti, Mg, C, La, Ce, Nb, Se, V, B, Si, Cr, Mn.

Ключевые слова: сталь, химический состав, аустенит, д-феррит, распределение элементов, дендрит, жидкий, фаза, твердый.

ВПЛИВ ТОВІЩИНИ СЛЯБІВ НА СЕГРЕГАЦІЮ ЕЛЕМЕНТІВ ПРИ БЕЗПЕРЕВНОМУ ЛИТТІ ЗАГОТОВОК С. Г. Афтанділянц

Анотація. У статті наводяться результати дослідження впливу товщини слябів на сегрегацію елементів при безперевному литті заготовок.

Розглянуто процес накопичення елементів на поверхні дендритів при кристалізації сталевих слябів різної товщини. Встановлено теоретична залежність процесу накопичення елементів на поверхні дендритів при кристалізації сталевих слябів різної товщини. Показано, що ефективність накопичення елементів на поверхні дендритів істотно залежить від швидкості кристалізації і охолодження сляба. Встановлена залежність дозволяє визначити допустимий підвищений вміст елементів в стрічках, еквівалентну їхнім змістом у товстих слябах при безперервному літті заготовок. Дослідження сегрегації елементів показало, що при розливання тонких сталевих стрічок можливе збільшення вмісту елементів в порівнянні з безперервним літтєм товстих слябів при ідентичному рівні сегрегації.

За рівнем максимального збільшення вмісту домішок в тонких стрічках з вуглецевої сталі AISI 1006 елементи розташовуються в наступній спадної послідовності: S, O, N, P, H. Для тонких стрічок з нержавіючої сталі AISI 304 спостерігається інша послідовність: O, S, P, H, N.

У разі залишкових елементів спостерігаються такі закономірності:

- для стрічки зі сталі AISI 1006 - Pb, Bi, Sn, As, Zn, Sb, Cu;
- стрічки зі сталі AISI 304 - Cu, Sb, Sn, Bi, Pb, As, Zn.

Для легуючих елементів послідовності мають такий вигляд:

- стрічки зі сталі AISI 1006 - B, Se, Al, Te, Ca, Mg, Ce, C, La, Nb, Ti, Mn, Ni, Si, Cr;
- стрічки зі сталі AISI 304 - Ca, Te, Al, Ti, Mg, C, La, Ce, Nb, Se, V, B, Si, Cr, Mn.

Ключові слова: сталь, хімічний склад, аустеніт, δ-ферит, розподіл елементів, дендрит, рідкий, фаза, твердий.

Є. Г. Афтанділянц ORCID 0000-0001-5864-9855.